Geophys. J. R. astr. Soc. (1979) **56**, 1–18

Asthenospheric counterflow: a kinematic model

Clement G. Chase *Department of Geology and Geophysics, University of Minnesota, Minneapolis, Minnesota 55455, USA*

Received 1978 March 7

Summary. Present-day plate motions imply that about 240 km^3 of oceanic lithosphere is created by sea-floor spreading and destroyed by subduction per year. A greater volume of asthenosphere will be dragged along by plate motions. Given the fluxes generated at plate boundaries, the horizontal direction and net rate of counterflow required to maintain mass balance is determined globally by a simple analytical model. Time-dependent calculations indicate that the motions are approximately valid in the hotspot reference frame over the past 5 Myr. Under most plates, the model return flow is opposite to the lithospheric motion in the hotspot frame. The counterflow dominates the resisting stresses to plate motion, so driving force models based on plate drag alone are not valid where the directions of plate motion and counterflow differ. The most marked departure of the two directions is under the North American plate. The model counterflow directions indicate that the sources of mantle hotspots are not located within the asthenosphere. Model flux balances demonstrate exchange of material between asthenospheric reservoirs located beneath different plates. Suggestions of southward asthenospheric motion under the North Atlantic, based on physical features around Iceland and strontium isotope geochemistry, are consistent with the direction of flow predicted by the model.

Introduction

It is ironical that the very rigidity and thermal inertia of lithospheric plates that make it possible to measure accurately their relative motion at the surface of the Earth also make it extremely difficult to determine the motions of the material below (McKenzie 1969). The relative surface motions for the past 5 or 10 Myr are now well known (Morgan 1972; Chase 1972; Minster *et al.* 1974; Chase 1978). If we allow that the mantle hotspots move more slowly with respect to the lower mantle or the Earth's rotational axis than the plates do, we can also obtain reasonable estimates of 'absolute motion' (Morgan 1972; Minster *et al.* 1974) or at least motion in a 'mean hotspot frame of reference' (Chase 1978).

The relative motions imply that sea-floor spreading generates about 3 $km^2\ yr^{-1}$ of new oceanic lithosphere (Chase 1972). An earth of constant radius then experiences destruction

of an equal area of lithosphere annually by subduction. With an average thickness of oceanic lithosphere of about 80 km (Press 1972), the volume flux of lithosphere must be about 240 $km^3 yr^{-1}$ (Chase 1976). The moving plates will also entrain asthenospheric material below by viscous drag. Clearly, a substantial counterflow at depth must exist to balance the volume flux of the lithosphere and of the asthenosphere that moves with it.

I will analyse here a simplified model of the counterflow to plate motions that permits calculation of at least the plan form or horizontal direction of the return flow. The difficulty of measuring mantle motions makes it hard to test the model at the present time. There is some geochemical evidence from the North Atlantic that tends to support the model. However, some of the implications of the model are clear. It makes the hypothesis that the source of mantle hotspots lies within the asthenospheric counterflow (McDougall 1971; Forristall 1974) unlikely. Estimates of the directions of stresses resisting plate motions can be improved over the simple viscous drag models (Solomon & Sleep 1974; Forsyth & Uyeda 1975). The model emphasizes the point of Garfunkel (1975) that circulation in the mantle cannot consist of simple closed cells, but that material is interchanged between the reservoirs underlying the individual plates. This may offer a partial explanation for the observation by Barazangi & Isacks (1976) of a very shallow dip of the Benioff zone under parts of South America.

There are two independent studies of asthenospheric counterflow, by Parmentier & Oliver (1978) and Hager & O'Connell (1978). Each starts from a different viewpoint than this one, but some conclusions seem common to all. It is beyond the scope of this paper, however, to discuss and compare the different assumptions and approaches of these other studies.

The model: assumptions

The aim is to construct a model that will serve as a first approximation to asthenospheric flow. The horizontal direction of the flow is to be determined by applying kinematic boundary conditions consisting of the flux of asthenosphere at plate boundaries caused by the creation or destruction of lithosphere and by the viscous flow entrained by motion of the plates. In this context the subduction zones become sources, by displacement, of asthenospheric material and the spreading centres act as sinks. Hotspots can also be easily accommodated as sources within the model.

The basic assumption is that asthenospheric motions take place within a spherical shell of constant and limited depth extent. It is clear that the plate motions must represent the upper part of a thermal convection system within the Earth. What is not clear is how deep this particular system extends. Several recent estimates of variation of mantle viscosity with depth would permit whole mantle convection (O'Connell 1977; Sammis *et al.* 1977; Davies 1977a), but a variety of evidence suggests that the counterflow should at least be concentrated in the upper mantle (Press 1972; McKenzie & Weiss 1975; Schubert *et al.* 1978). The present model is not particularly sensitive to the depth used for the bottom of the asthenosphere, which appears only in scale factors. A slowly varying asthenospheric thickness can be accommodated by scaling the velocities calculated from the model (Preston 1965). The asthenosphere is also assumed to have constant Newtonian viscosity. A more complicated radial viscosity distribution will affect the magnitude but not the direction of the velocity and stress results.

Most of the remaining assumptions spring from the extremely low Reynolds number of the mantle. This number, which describes the ratio of inertial to viscous forces, will be considerably smaller than 10^{-10} for reasonable velocities and viscosities. In effect, the mantle

has no mechanical memory at all, only thermal and chemical memories. These latter will not be modelled here, and I will put aside for the moment the question of 'two-scale convection' (Richter 1973; McKenzie & Weiss 1975) in which the return flow has superimposed upon it local convection cells or rolls. Within these limitations the model mantle is extremely compliant and the velocities cannot exhibit transient behaviour, but adjust instantly to changes in the boundary conditions.

The flow is assumed to be horizontal away from the sources and sinks. Numerical studies of circulation in a viscous layer driven by motion of the top surface (Davies 1977b) show that the flow will be dominantly horizontal at distances from the lateral boundaries greater than the depth of the layer. Calculations by Hager & O'Connell (1976, 1978) of plate-driven return flow suggest that vertical motion may persist to considerable depths but the details depend on the viscosity model. Finally, the flow is treated as incompressible.

SHEAR OR ENTRAINED FLOW

The starting point for the boundary conditions is a set of relative plate motions (Chase 1978) that gives the amount of lithosphere being created or destroyed at the plate boundaries. For these calculations, a constant thickness of 80 km is taken for the lithosphere. The next consideration is the viscous flow induced by motion of the plates over an assumed stationary lower mantle. These 'absolute' motions are approximated by motions in the mean hotspot frame of reference (Chase 1978). The theory of shear flow between concentric shells at low Reynolds numbers is straightforward (Landau & Lifshitz 1959).

This shear-induced or entrained flow enters into the calculation in two ways. The plates drag the asthenosphere away from ridges and toward trenches, which increases the fluxes generated at the plate boundaries. The counterflow must balance this increased flux, which fortunately is proportional to the relative plate velocities. In the spherical geometry used here, the mean asthenospheric velocity will be slightly less than half the lithospheric velocity (Appendix A), and the flux will be proportional to the asthenospheric thickness. For an asthenosphere bottoming at 350 km the shear flow already represents 60 per cent of the flux that must be balanced by the counterflow. For a 700-km deep asthenosphere, the shear flow is 80 per cent of the total. These estimates are for uniform viscosity. If the viscosity varies with depth, the shear gradient will be strongly concentrated at the level of minimum viscosity (Schubert & Turcotte 1972).

Under the assumptions above, the shear flow can be calculated both as a function of position on the Earth and as a function of depth (Fig. 1). The equations governing this flow are linear and uncoupled to the counterflow equations, so either the mean velocities or the velocity at any depth can be linearly superposed upon the counterflow to give the net asthenospheric motion. This can be vectorially added to the plate motions to calculate relative motion of asthenosphere versus lithosphere.

THE RETURN FLOW

The other kind of flow that must be calculated is the counterflow proper. Here a remarkable approximation is available for incompressible flow at low Reynolds numbers. Consider the planar case, in which we have viscous flow between parallel walls. The walls must be close enough together so that the lateral variation of the velocity of flow is small compared to its vertical variation due to viscous shear against the walls. This is a good approximation for the asthenosphere away from the sources and sinks. The mean velocity of flow is then derivable from a potential that satisfies LaPlace's equation (Lamb 1945). Thus the mean velocity

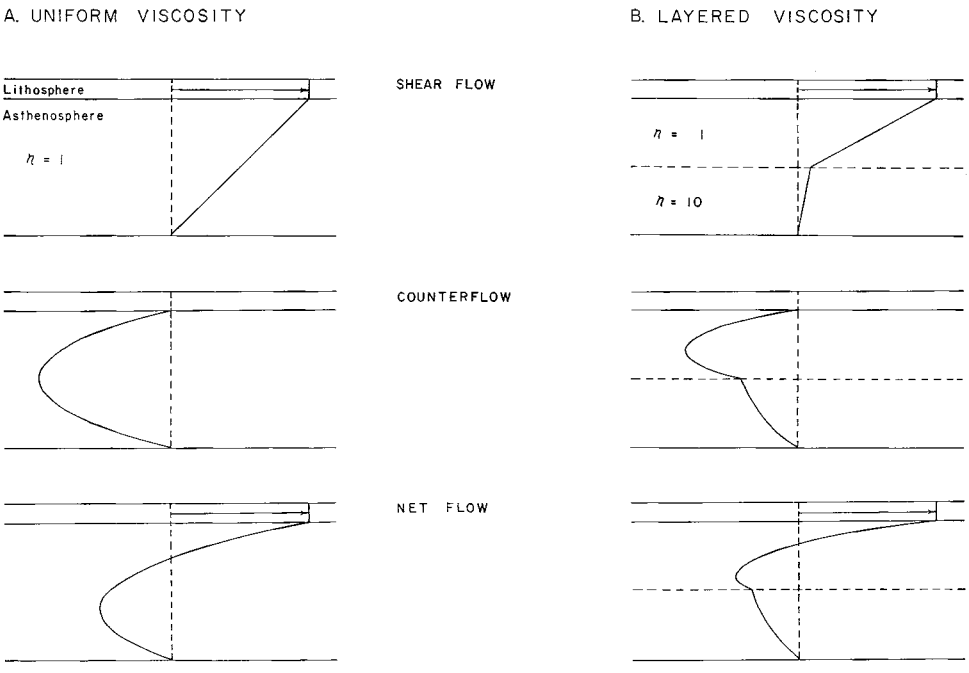

Figure 1. Simple models of vertical variation of velocity for shear (drag) flow and counterflow, planar one-dimensional model. In both cases A and B, the shear stress due to return flow is approximately four times that due to the entrained shear flow. (A) Asthenosphere of uniform Newtonian viscosity. (B) Viscosity in lower half of asthenosphere is 10 times that in the upper half, the mean viscosity is 5.5 times that of case (A). Compared to case (A), the shear stress is doubled and the horizontal pressure gradient associated with the counterflow is quadrupled. The lateral pressure gradient is the same in both the upper and lower halves of the asthenosphere.

reduces to a two-dimensional potential flow and the horizontal direction of flow is irrotational. Given the mean velocity, the vertical variation of velocity (Fig. 1) can be obtained from its parabolic form between the stationary walls (Lamb 1945). This flow is termed Hele–Shaw flow, and its use has been largely restricted to laboratory demonstrations of potential flow.

Hele–Shaw flow is easily adapted to a spherical shell and calculable from kinematic boundary conditions of source and sink strength and distribution. For a single point source generating a flux of $f\,\mathrm{km^3\,yr^{-1}}$, the mean horizontal velocity is directed tangentially away from the source with a speed proportional to $f(4\pi)^{-1}\cot(\theta/2)$, where θ is the central angle between the source and the point of observation (see Appendix A). The source is, in effect, a vertical line source spanning the asthenosphere. The solution is unique given symmetry of the flow and boundedness at the antipode of the source. The divergence of this flow is proportional to f and constant independent of position on the sphere, except at the source, where it is opposite. Therefore, an equal total strength of sources and sinks gives a flow that satisfies conservation of mass. The flows due to separate sources and sinks are linearly superposable, and the net counterflow is superposable upon the shear-induced drag flow. The vertical variation of the Hele–Shaw flow can be calculated from the condition of zero slip at the spherical boundaries (Fig. 1).

It should be noted that, subject to symmetry of flow due to a point source and knowledge of the fluxes generated by plate motions, the Hele–Shaw flow gives with

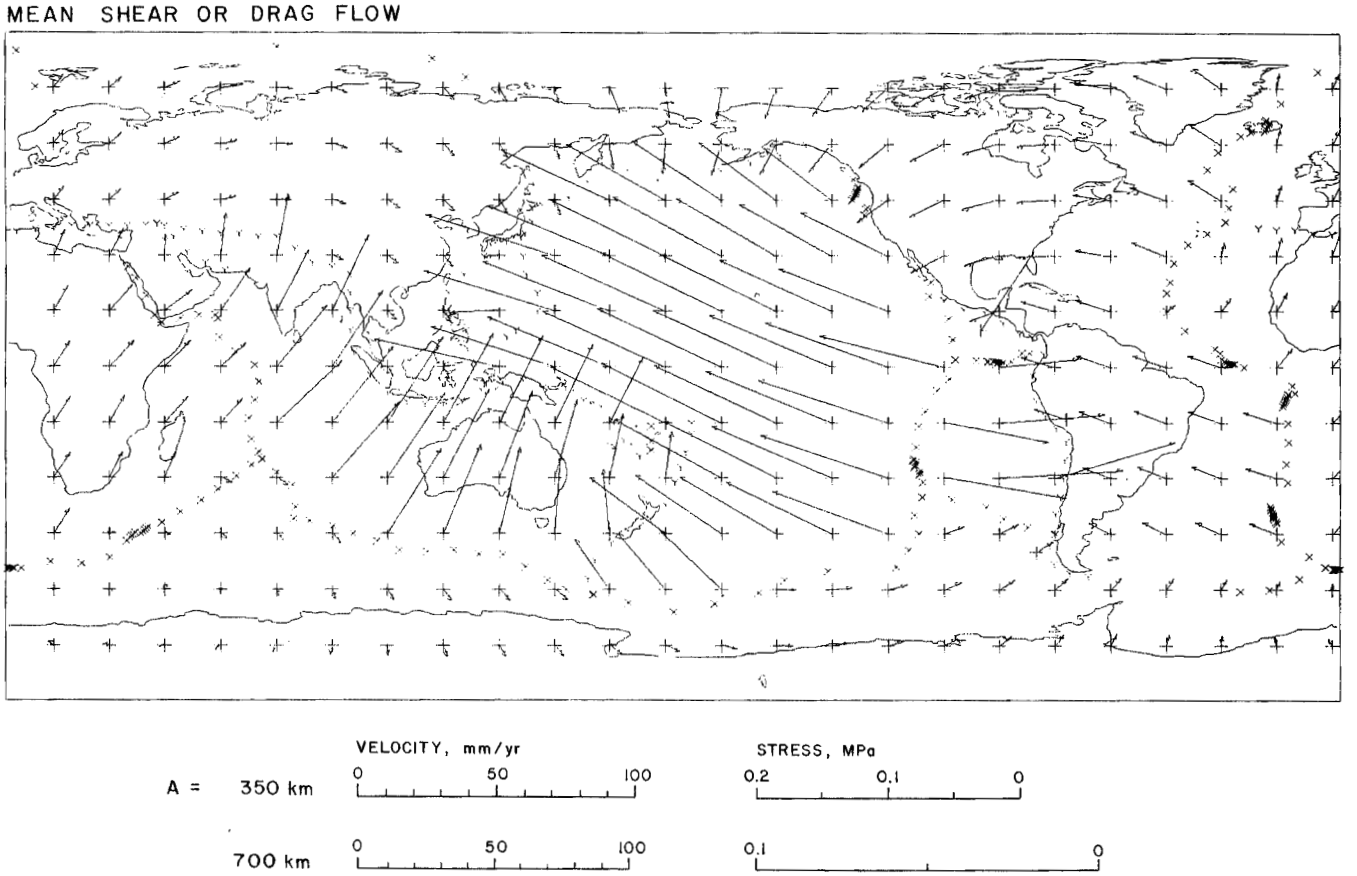

Figure 2. Mean drag or shear flow velocity for plate motions in 'mean hotspot frame' (Chase 1978). The mean drag flow velocity is about half the velocity of the overlying plate. 'X' marks the digitized point on spreading centre (sink) and 'Y' marks the subduction zone (source). Scales give velocity and shear stress on plate for depth to bottom of asthenosphere A = 350 and 700 km. Stress scales are reversed because the shear stress exerted on the overlying plate is in the opposite direction to the velocity. The stresses are based on a viscosity of 10^{19} Pa s (pascal second, 1 Pa s = 1 N s m^{-2} = 10 poise). Plate thickness 80 km. Cylindrical equidistant projection.

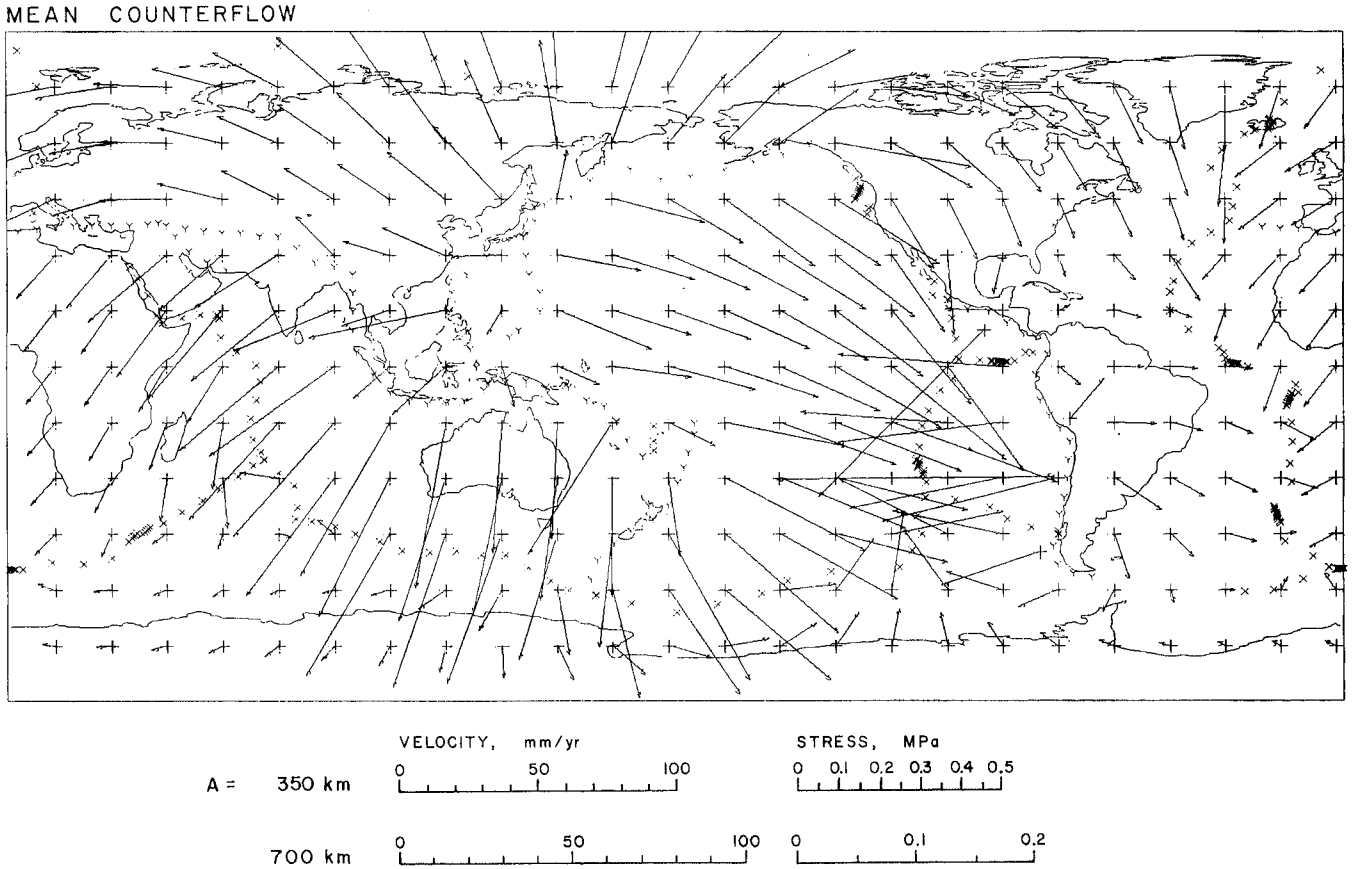

Figure 3. Mean asthenospheric counterflow velocity for relative motion model P071 (Chase 1978). This flow balances the plate flux and entrained shear flow. Scales are for two asthenospheric depths. Shear stresses exerted on overlying plates are in same direction as return flow. Viscosity, symbols as in Fig. 2.

complete generality the net flux across any vertical surface spanning the region of counterflow. This is true even if secondary convection rolls are active, and does not depend upon the depth of the convective system.

In contrast to the shear flow, there is a pressure gradient associated with the return flow (Appendix A), see later. In addition, the counterflow is less strongly channelled into regions of low viscosity (Fig. 1), an effect that explains the penetration of the flow into deeper layers in the models of Hager & O'Connell (1976, 1978).

Results of the model

The distribution of ridges and trenches was approximated by the sinks and sources shown on Figs 2 to 5 by Xs and Ys, respectively, and the appropriate fluxes assigned to these points using the relative motion model of Chase (1978). In this study, hotspots were not used as sources, although they would be easily accommodated. Fig. 2 displays the mean shear or drag flow calculated from plate motions in the mean hotspot reference frame (Chase 1978), an approximation to a lower mantle at rest. The stresses exerted on the overlying plate are proportional to the velocity and in the opposite direction. The stresses are also proportional to the viscosity of the asthenosphere, which was taken as 10^{19} Pa s (pascal second, 1 Pa s = 10 poise) for the shear stress scales shown in the figures. Fig. 3 shows the model counterflow velocities necessary to balance the flux of lithosphere and drag flow at the plate boundaries. Here the stresses are in the same direction as the mean return flow velocity.

COORDINATE SYSTEM

The question immediately arises: in what reference frame are the counterflow velocities represented? They are instantaneous velocities, relative to the instantaneous distribution of plate boundaries. However, the boundaries and the flow are constantly evolving and the particle motions would *not* follow streamlines, had those been calculated. A test was carried out in which the plate boundaries were moved back in steps to their positions 5 Myr ago in the hotspot reference frame. The particle motions for each step at a number of sites were calculated, and the net motions compared to the instantaneous velocities of Fig. 3. In the regions where the model is most valid, away from the plate boundaries, the agreement was good, rates within 5 per cent, directions within 5°. Thus the motions are valid as velocities in the hotspot frame over the last 5 Myr.

STRESSES ON PLATES

Comparing Figs 2 and 3, the striking result is that under most plates the drag flow and the counterflow are in nearly opposite directions (Chase 1976). This has a number of important consequences. One is that one-dimensional models of the flow are adequate in many places. Counterflow dominates the stresses on the over-lying plates in this model, being several times as effective at producing resisting stresses as the shear-induced drag for a 700-km deep asthenosphere (see Appendix). Driving force and plate stress calculations that use the viscous drag as a resisting force to plate motion (Solomon & Sleep 1974; Forsyth & Uyeda 1975; Solomon, Sleep & Richardson 1975; Harper 1975; Richardson, Solomon & Sleep 1976) are adequate *only* for the plates under which the counterflow stresses parallel the stresses caused by viscous drag over the lower mantle. The driving force models scale the driving to the resistive forces, so the difference in magnitude between shear flow and return flow

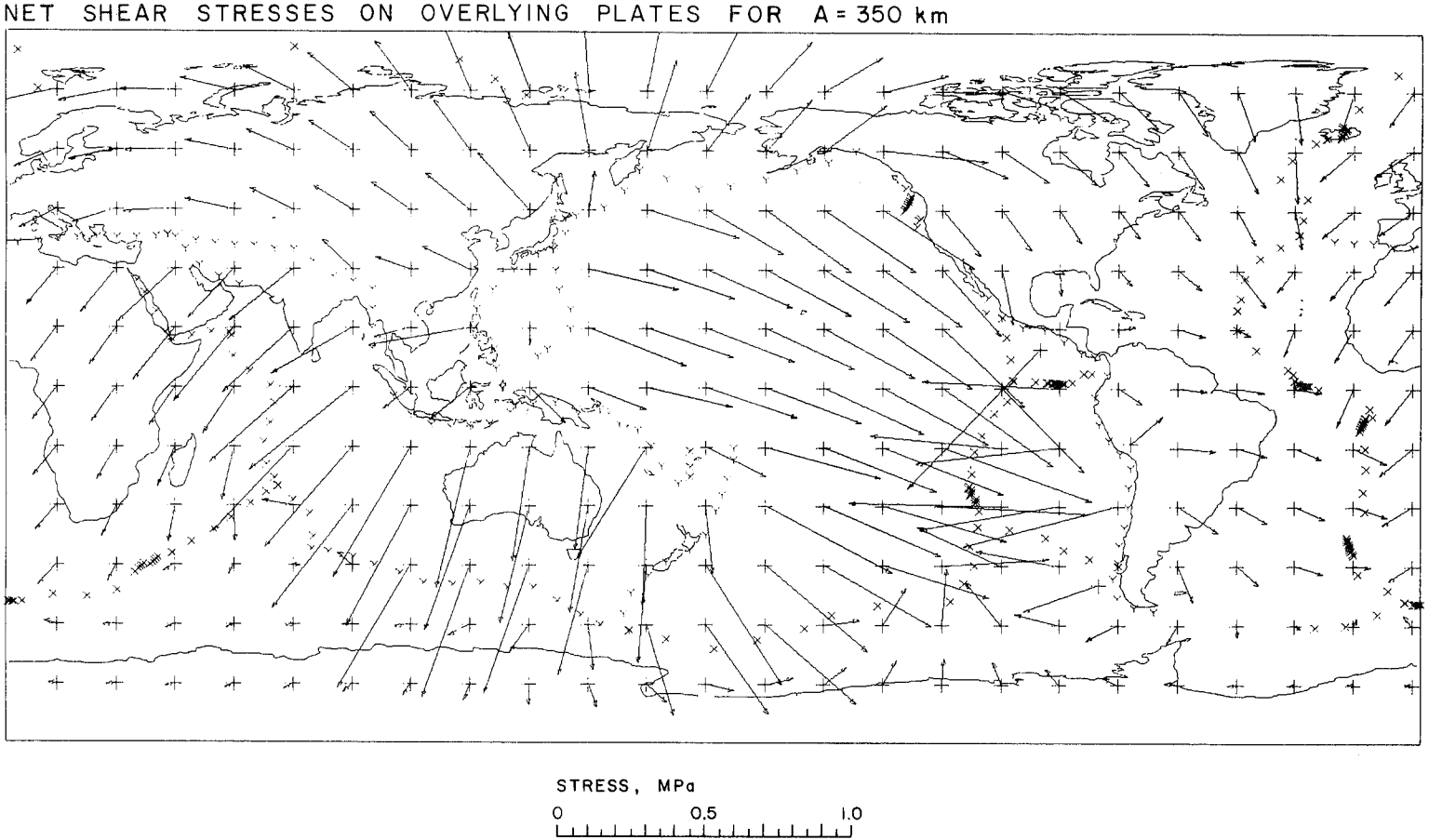

Figure 4. Total shear stress exerted on the overlying plates by the shear and return flows, asthenospheric depth 350 km. Note that the stress directions are similar to the counterflow (Fig. 3). Assumed viscosity 10^{19} Pa s.

stresses would not cause a significant change in the result if they are parallel. The North American plate shows the greatest divergence in direction of return flow and shear flow – compare Figs 2 and 3, and Fig. 4, which represents the net stresses for a 350-km deep asthenosphere, viscosity 10^{19} Pa s. For this particular plate, the site of many of the existing intraplate stress estimates, the viscous drag over the lower mantle will not suffice as a model of the forces resisting motion.

There is nothing in this model to explain the driving forces themselves, because the flow is driven exclusively by the plate motions. In the case of plates with a significant amount of subducting slab attached, one can appeal to pull by the downgoing lithosphere to drive the plate motion. In the case of the plates surrounding the Atlantic Ocean, the problem of driving forces is not so easily evaded. Either the opening of the Atlantic is driven by forces originating within the plates, namely sliding off the ridges, or the pattern of motion shown in Fig. 3 cannot be accurate in detail. The stresses in the counterflow model only resist Atlantic spreading. Whether the missing driving force is trench suction (Forsyth & Uyeda 1975), hotspot drive (Morgan 1972), ridge push or something else is not yet clear.

SOURCES OF THE HOTSPOTS

One of the original motives of this project was to test the hypothesis that the source region for the mantle hotspots is located within the zone of asthenospheric return flow (McDougall 1971; Forristall 1974). Within the mean hotspots frame of reference, there is some misfit of the direction of the hotspot traces (Minster *et al.* 1974; Chase 1978). Thus I wanted to see if asthenospheric motion would explain the misfit. There are two difficulties in testing this idea. One is that directions of the hotspot traces are much better known than rates of progression of volcanism along them, so we have only one component of the misfit vector (Chase 1978). The other is that flow in the model asthenosphere varies in both direction and magnitude as a function of depth (Fig. 1), and it is not obvious just where within the flow the hotspot source might be located.

Taking these problems into account, the best test that could be devised was to consider whether *any* component of the counterflow added to the mean hotspot frame motions could improve the fit. The results were mixed, but on the whole negative. Three of the hotspot directions out of 20 listed by Minster *et al.* (1974) needed no improvement – Hawaii, Juan de Fuca and McDonald on the Pacific plate. Two fits would be improved by some component of counterflow – Easter trace on Nazca plate, Prince Edward Island trace on the Antarctic plate. Five might be improved by a slight contribution from counterflow – Iceland and Yellowstone on the North American plate, Easter on the Pacific plate, Tristan du Cunha on the South American plate, Iceland on the Eurasian plate. For the remaining 10, the fit of the hotspot frame would only be degraded if the hotspots experienced any component of the model asthenospheric counterflow.

These results strongly suggest that most hotspots sources are not affected by any flow that resembles this model. Other cogent reasons exist why the sources for the hotspots cannot persist within the asthenosphere. The hydrodynamic dispersion caused by the shearing within a thin asthenosphere would soon erase anything distinctive about a mantle melting anomaly. It is interesting to note, however, a curious correspondence between hotspots located away from spreading centres and the net flow (vector sum of mean shear flow and mean counterflow) show in Fig. 5. Many of the hotspot locations, shown by open circles in Fig. 5, are in areas where the net motion of material in the asthenosphere is close to zero. I will not attempt to speculate here as to the reasons for this correspondence.

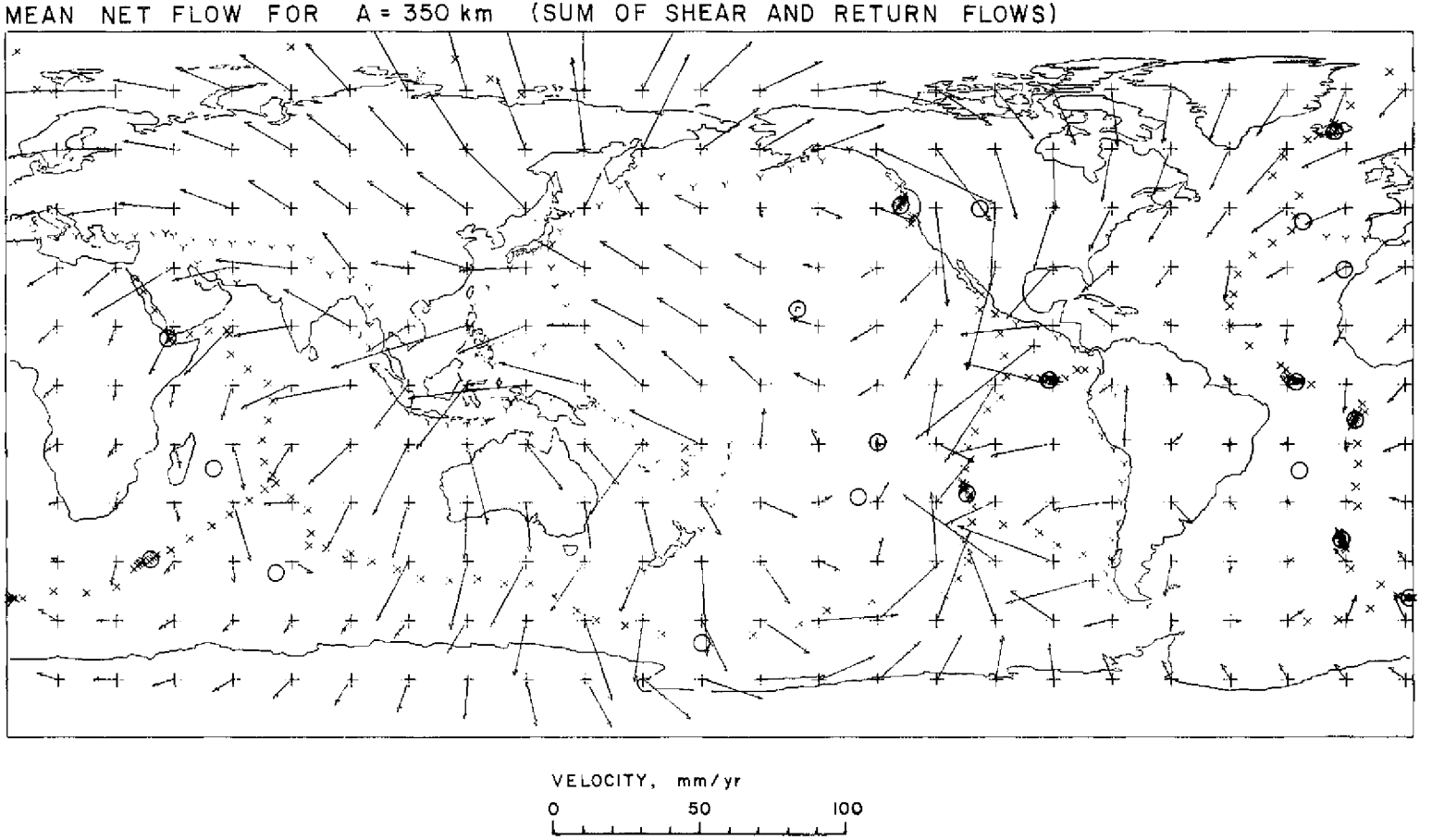

Figure 5. Net flow (vector sum of Figs 2 and 3) for an asthenosphere with bottom at 350 km. The open circles mark the locations of some of the more vigorous hotspots.

INTERCONNECTED ASTHENOSPHERIC RESERVOIRS

As noted by Garfunkel (1975) the long-term effects of plate motion imply that circulation in the mantle cannot occur in simple closed cells. For example, the growth of the Atlantic and Indian Oceans at the expense of the Pacific means that asthenosphere must be displaced from beneath the Pacific. The counterflow model can give an instantaneous picture of this displacement process. The balance of plate, shear-induced, and return fluxes was calculated for segments of a number of plate boundaries, of which I will discuss two.

The flux balance for the Peru–Chile trench indicates that most of the asthenosphere displaced by the subducted slab should move towards the South Atlantic, together with the material delivered by drag of the South American plate. The shear flow dragged in by the Nazca plate is needed at the East Pacific Rise. However, the Peru–Chile trench partakes of the westward motion of South America in the mean hotspot reference frame (Fig. 2). Following the argument of Garfunkel (1975), there should be an additional eastward flow below the plates to allow the westward retreat of the subducted slab. The tendency for flow across the convergence zone from west to east may offer a partial explanation for the extremely shallow dips of the Benioff zone in some places under South America (Barazangi & Isacks 1976). One might say that the downgoing slab is being blown out of the way of the mantle flow.

In the eastern Aleutian trench, where there is a well-developed Benioff zone, the flow needed to supply the spreading centres in the North Atlantic is parallel to the trench on the North American side (Fig. 5), and the net flow under the Pacific plate is to the south, allowing for southward motion of the trench in the hotspot frame (Fig. 2). Further west, the plate boundary becomes parallel to the North American/Pacific relative plate motion, and the Benioff zone vanishes. In this region the net flux is northward from underneath the Pacific plate through the 'pass' created by the strike-slip segment of the plate boundary (Fig. 5). Thus the Atlantic asthenosphere is replenished by material lost from the Pacific, and the two mantle reservoirs are intermingled. Similar exchanges of material take place at other plate boundaries.

Discussion

The simplifications incorporated in this model of asthenospheric counterflow limit its range of applicability. In particular, restriction of the calculation to horizontal flow means that the velocities cannot be valid nearer to the plate boundaries than the depth of the convecting system. If that depth is small, the model should be approximately correct away from the plate boundaries. The requirements of mass balance are so stringent that this simple model should contain the essential features of the actual flow.

If small-scale convection within the asthenosphere is necessary to dispose of radioactive heat generated deeper within the Earth (Richter 1973; Richter & Parsons 1975; McKenzie & Weiss 1975), then the patterns of flow calculated here can only be taken as net flux through vertical surfaces. The conclusion that hotspot sources are not located within the counterflow is then weakened. The calculations of flux balances are not strongly affected, however.

Another problem is connected with the pressure gradients necessary to drive the return flow. These pressure gradients imply elevation gradients away from subduction zones towards spreading centres, the opposite of the observed case (Schubert & Turcotte 1972). If the viscosity of the asthenosphere is as low as the value used for Figs 2, 3 and 4, the gradients are not large enough to be observable. For a higher viscosity, the cooling of oceanic

lithosphere can more than balance the pressure gradients (Schubert *et al.* 1978), although no such explanation is available for the continental lithosphere. A much better knowledge of the viscosity profile of the mantle is needed to resolve this problem.

Given these difficulties, the most appealing test of the counterflow model would be one based on evidence completely independent from that on which the model is based. Bathymetric (Vogt 1971) and geochemical data from the North Atlantic may offer such a test. There are a number of hotspots on the Mid-Atlantic Ridge in the North Atlantic that represent an excess of magma over that poured out at normal segments of the ridge. In particular, Iceland and the Azores show clear evidence of hotspot activity. It is now well known that hotspot (oceanic island) magmas have a distinctive trace element composition compared to normal ridge basalts (Gast, Tilton & Hedge 1964; Schilling 1973; Hofmann & Hart 1975; Sun & Hanson 1975 and others). The most important characteristic here is the high initial $^{87}Sr/^{86}Sr$ ratio of oceanic island basalts, which is unlikely to be affected by fractional crystallization. Diffusion of strontium in a partially molten mantle is likely to be fast enough that high initial strontium ratios cannot be caused by disequilibrium melting (Hofmann & Hart 1975). Therefore the high strontium ratios are probably characteristic of the mantle from which hotspots are derived, in contrast to the lower ratios of normal suboceanic mantle. This means that the strontium ratios can be used as a tracer of mantle motions.

As one goes north on the Mid-Atlantic Ridge from about 20° N, the initial strontium ratios of basalts dredged from the ridge crest increases gradually until a peak is reached where the Azores platform intersects the ridge, and then fall off abruptly to the north (White, Schilling & Hart 1976). Further north along the ridge, initial strontium again rises gradually towards Iceland (Schilling 1973; Hart, Schilling & Powell 1973). Strontium data are not yet available from just north of Iceland, but La/Sm ratios there are typical of normal mid-oceanic basalts (W. M. White 1977, private communication), suggesting lack of hotspot contribution. In both cases, the geochemical 'tail' of the hotspot extends to the south. Thus the strontium data suggest flow, probably shallow, to the south along the ridge axis. This same conclusion was reached by Vogt (1971, 1976) and Vogt & Johnson (1975), primarily on physiographic grounds. Now note that in Figs 3 and 5, the predicted direction of mantle flow is southward in the North Atlantic. This simplified model of shallow return flow agrees well with at least one external test.

Acknowledgments

The development of the ideas contained herein was aided by discussions with H. O. Pfannkuch, R. Shreve, V. R. Murthy, R. Aris, W. M. White and many others. Especial thanks to M. Brandt for carrying out many of the computations and checking the equations. This work was supported by National Science Foundation grant EAR 75-21622.

References

Barazangi, M. & Isacks, B. L., 1976. Spatial distribution of earthquakes and subduction of the Nazca plate beneath South America, *Geology*, **4**, 686–692.

Chase, C. G., 1972. The *n*-plate problem of plate tectonics, *Geophys. J. R. astr. Soc.*, **29**, 117–122.

Chase, C. G., 1976. Asthenospheric counterflow: a kinematic model (abstract), *EOS, Trans. Am. Geophys. Un.*, **57**, 1002.

Chase, C. G., 1978. Plate kinematics: the Americas, East Africa and the rest of the world, *Earth planet. Sci. Lett.*, **37**, 355–368.

Davies, G. F., 1977a. Whole-mantle convection and plate tectonics, *Geophys. J. R. astr. Soc.*, **49**, 459–486.

Davies, G. F., 1977b. Viscous mantle flow under moving lithospheric plates and under subduction zones, *Geophys. J. R. astr. Soc.*, **49**, 557–563.

Forristall, G. Z., 1974. The thickness of the asthenosphere deduced from the motion of the Hawaiian hot spots, *Geophys. Res. Lett.*, **1**, 131–133.

Forsyth, D. & Uyeda, S., 1975. On the relative importance of the driving forces of plate motion, *Geophys. J. R. astr. Soc.*, **43**, 163–200.

Garfunkel, Z., 1975. Growth, shrinking and long term evolution of plates and their implications for the flow pattern in the mantle, *J. geophys. Res.*, **80**, 4425–4432.

Gast, P. W., Tilton, G. R. & Hedge, C., 1964. Isotropic composition of Pb and Sr from Ascension and Gough islands, *Science*, **145**, 1181–1185.

Hager, B. H. & O'Connell, R. J., 1976. Viscous flow in the mantle driven by moving plates (abstract), *EOS, Trans. Am. Geophys. Un.*, **57**, 1002–1003.

Hager, B. H. & O'Connell, R. J., 1978. Kinematic models of large scale flow in the earth driven by the moving plates, *J. geophys. Res.*, in press.

Harper, J. F., 1975. On the driving forces of plate tectonics, *Geophys. J. R. astr. Soc.*, **40**, 465–474.

Hart, S. R., Schilling, J. R. & Powell, J. L., 1973. Basalts from Iceland and along the Reykjanes Ridge, Sr isotope geochemistry, *Nature Phys. Sci.*, **264**, 104–107.

Hofmann, A. W. & Hart, S. R., 1975. An assessment of local and regional isotopic equilibrium in a partially molten mantle, *Carnegie Inst. Wash. yr Book*, **74**, 195–210.

Lamb, H., 1945. *Hydrodynamics*, 6th edn, Dover, New York.

Landau, L. P. & Lifshitz, E. M., 1959. *Fluid Mechanics*, Addison-Wesley, Reading, Massachusetts.

McDougall, I., 1971. Volcanic island chains and sea floor spreading, *Nature*, **231**, 141–144.

McKenzie, D. P., 1969. Speculations on the consequences and causes of plate motions, *Geophys. J. R. astr. Soc.*, **18**, 1–32.

McKenzie, D. & Weiss, N., 1975. Speculations on the thermal and tectonic history of the earth, *Geophys. J. R. astr. Soc.*, **42**, 131–174.

Minster, J. B., Jordan, T. H., Molnar, P. & Haines, E., 1974. Numerical modelling of instantaneous plate tectonics, *Geophys. J. R. astr. Soc.*, **36**, 541–576.

Morgan, W. J., 1972. Plate motions and deep mantle convection, *Geol. Soc. Am. Mem.*, **132**, 7–22.

O'Connell, R. J., 1977. On the scale of mantle convection, *Tectonophys.*, **38**, 119–136.

Parmentier, E. M. & Oliver, J. E., 1978. A study of shallow global mantle flow due to the accretion and subduction of lithospheric plates, *Geophys. J.*, in press.

Press, F., 1972. The earth's interior as inferred from a family of models, pp. 147–171, in *The Nature of the Solid Earth*, ed. Robertson, E. C., McGraw-Hill, New York.

Preston, J. H., 1965. Extensions of the Hele–Shaw analogy, pp. A1–A23, in *Proc. Australasian Conf. Hydraulics Fluid Mech.*, 2nd, Auckland, New Zealand.

Richardson, R. M., Solomon, S. C. & Sleep, N. H., 1976. Intraplate stress as an indicator of plate tectonic driving forces, *J. geophys. Res.*, **81**, 1847–1856.

Richter, F. M., 1973. Convection and large-scale circulation of the mantle, *J. geophys. Res.*, **78**, 8735–8745.

Richter, F. M. & Parsons, B., 1975. On the interaction of the two scales of convection in the mantle, *J. geophys. Res.*, **80**, 2529–2541.

Sammis, C. G., Smith, J. C., Schubert, G. & Yuen, D. A., 1977. Viscosity-depth profile of the earth's mantle: effects of polymorphic phase transitions, *J. geophys. Res.*, **82**, 3747–3761.

Schilling, J. G., 1973. Iceland mantle plume: geochemical study of Reykjanes Ridge, *Nature*, **242**, 565–571.

Schubert, G. & Turcotte, D. L., 1972. One dimensional model of shallow-mantle convection, *J. geophys. Res.*, **77**, 945–951.

Schubert, G., Yuen, D. A., Froidevaux, C. & Souriau, M., 1978. Mantle circulation with partial shallow return flow, *J. geophys. Res.*, in press.

Solomon, S. C. & Sleep, N. H., 1974. Some simple physical models for absolute plate motions, *J. geophys. Res.*, **79**, 2557–2567.

Solomon, S. C., Sleep, N. H. & Richardson, R. M., 1975. On the forces driving plate tectonics: inferences from absolute plate velocities and intraplate stress, *Geophys. J. R. astr. Soc.*, **42**, 769–801.

Sun, S. C. & Hanson, G. R., 1975. Evolution of the mantle: geochemical evidence for alkali basalt, *Geology*, **3**, 297–302.

Vogt, P. R., 1971. Asthenosphere motion recorded by the ocean floor south of Iceland, *Earth planet. Sci. Lett.*, **13**, 153–160.

Vogt, P. R., 1976. Plumes, subaxial pipe flow, and topography along the mid-oceanic ridge, *Earth planet. Sci. Lett.*, **29**, 309–325.

Vogt, R. P. & Johnson, G. L., 1975. Transform faults and longitudinal flow below the mid-oceanic ridge, *J. geophys. Res.*, **80**, 1399–1428.

White, W. M., Schilling, J. G. & Hart, S. R., 1976. Evidence for the Azores mantle plume from strontium isotope geochemistry of the central North Atlantic, *Nature*, **263**, 659–663.

Appendix A: counterflow theory: general assumptions

We assume an asthenosphere of constant thickness and constant Newtonian viscosity. Define: c = radius of spherical earth, b = radius of lithosphere/asthenosphere boundary, a = radius of bottom of asthenosphere. We neglect gravity and thermal effects and assume that the flow is steady, has a very small Reynolds number (so that viscosity forces dominate) and is incompressible and has no vertical components. This is a nice, simple, orderly world we are modelling.

THE FLUXES WE NEED TO BALANCE

Volume flux of the lithosphere (plate flux). Flux induced by lithosphere motion by viscous drag (shear flux).

Let us assume motion of one plate relative to another fixed plate described by angular velocity $\boldsymbol{\omega}$, and choose the north pole of coordinate system $[\theta\,(\text{colat}), \phi(\text{long}), r(\text{radius})]$ parallel to $\boldsymbol{\omega}$, and calculate the flux due to the segment of plate boundary between co-latitudes θ_1 and θ_2.

Unit vectors $\hat{\mathbf{e}}_\theta$(south), $\hat{\mathbf{e}}_\phi$(east), $\hat{\mathbf{e}}_r$(up) at (θ, ϕ, r)

$\omega = |\boldsymbol{\omega}|$.

Plate flux = f_p

$$f_p = \pm \int_b^c \int_{\theta_1}^{\theta_2} |\boldsymbol{\omega} \times \mathbf{r}|\, r\,d\theta\,dr$$

$$= \omega \int_b^c \int_{\theta_1}^{\theta_2} \sin\theta\, d\theta\, r^2\, dr$$

$$f_p = \alpha\omega\,|\cos\theta_1 - \cos\theta_2|\left(\frac{c^3 - b^3}{3}\right) \qquad \text{(A1)}$$

f_p positive for convergent plate boundaries (asthenospheric sources), thus $\alpha = +1$, f_p negative for divergent plate boundaries (asthenospheric sinks), therefore $\alpha = -1$.

Shear flux = f_s

$$\mathbf{v}_s(\mathbf{r}) = \left(\frac{a^3 b^3}{b^3 - a^3}\right)(a^{-3} - r^{-3})\,(\boldsymbol{\omega} \times \mathbf{r})$$

(Landau & Lifshitz 1959)

$$= \left(\frac{a^3 b^3}{b^3 - a^3}\right)(a^{-3} - r^{-3})\,\omega r \sin\theta\,\hat{\mathbf{e}}_\phi$$

$$f_s = \int_a^b \int_{\theta_1}^{\theta_2} |\mathbf{v}_s(\mathbf{r})| r d\theta dr = \left(\frac{a^3 b^3}{b^3 - a^3}\right) \omega \int_{\theta_1}^{\theta_2} \sin\theta d\theta \int_a^b \left(\frac{r^2}{a^3} - \frac{1}{r}\right) dr.$$

With the same sign convention,

$$f_s = \alpha\omega |\cos\theta_1 - \cos\theta_2| \left(\frac{a^3 b^3}{b^3 - a^3}\right)\left[\frac{b^3 - a^3}{3a^3} - \ln\left(\frac{b}{a}\right)\right]. \tag{A2}$$

There are no pressure gradients associated with $\mathbf{v}_s$, and it satisfies $\nabla \cdot \mathbf{v}_s = 0$.
Mean shear flow velocity = $\bar{v}_\phi$

$$\bar{v}_\phi = \lim_{\Delta\theta \to 0} \frac{\iint f_s ds}{\int_a^b \int_{\theta_1}^{\theta_2} ds}$$

$$= \omega \sin\theta \left(\frac{2}{b^2 - a^2}\right)\left[\frac{b^3}{3} - \left(\frac{a^3 b^3}{b^3 - a^3}\right) \cdot \ln\left(\frac{b}{a}\right)\right].$$

Total flux f

$f = f_p + f_s$, adding (A1) and (A2)

$$f = \alpha\omega |\cos\theta_1 - \cos\theta_2| \left[\frac{c^3}{3} - \left(\frac{a^3 b^3}{b^3 - a^3}\right) \ln\left(\frac{b}{a}\right)\right]. \tag{A3}$$

THE COUNTERFLOW: HELE–SHAW FLOW ON A SPHERE

Kinematic conditions

For the entire counterflow, we require $\nabla \cdot \mathbf{v}_c = 0$. This we can ensure by requiring that the sum of the strengths $f_{(+)}$ of the sources equals the sum of $f_{(-)}$ of the sinks (mass balance). The conditions of the model guarantee that the flows caused by the individual sources and sinks are superimposable since the equations used below are linear in $\mathbf{v}$. We can then satisfy conservation of mass by requiring that, for a single source of sink,

$$\nabla \cdot \mathbf{v} \neq \text{function of } \theta, \phi \tag{A4}$$

and that

$$-\iint \nabla \cdot \mathbf{v} \; dV = \text{constant} \times f. \tag{A5}$$

Our sources now become vertical line sources spanning the thickness of the asthenosphere, approximating each segment of plate boundary by a point. Placing our 'point' source at $\theta = 0$, the north pole, symmetry requires that $v_\phi = 0$. We now impose our last assumption, that $v_r = 0$ so that we are dealing with pure horizontal flow.

$$\nabla \cdot \mathbf{v} = \frac{1}{r \sin\theta} \frac{\partial}{\partial\theta}(\sin\theta v_\theta) = \kappa(r)$$

$$\kappa(r) = \frac{1}{r \sin\theta}\left(\sin\theta \frac{\partial v_\theta}{\partial\theta} + \cos\theta v_\theta\right)$$

$$\frac{\partial v_\theta}{\partial \theta} + \cot\theta v_\theta = r\kappa(r). \tag{A6}$$

Solving by standard techniques with integration constant k_1,

$$v_\theta = \frac{-r\kappa(r)\cos\theta + k_1}{\sin\theta}.$$

To maintain boundedness at $\theta = \pi$ (south pole)

$$k_1 = -r\kappa(r)$$

$$v_\theta = -r\kappa(r)\left(\frac{1+\cos\theta}{\sin\theta}\right)$$

$$v_\theta = -r\kappa(r)\cot\left(\frac{\theta}{2}\right). \tag{A7}$$

Condition (A4) above is now satisfied, *without having specified the rheology at all.* By integrating (A7) and equating it to (A3), the condition (A5) can be satisfied for the mean velocity $\bar{v}_\theta$, but we want also the radial dependence of v_θ, which we will get from the:

Constitutive equation: Stokes equation

Under the various assumptions above,

$$\eta\nabla^2\mathbf{v} - \nabla P = 0 \tag{A8}$$

η = viscosity, $\mathbf{v}$ = velocity, P = pressure.

With a thin asthenosphere, v_r can be neglected away from the plate boundaries, and for our simple case, v_ϕ is excluded by symmetry. Thus we need consider only the θ component of (A8).

$$\frac{1}{r}\frac{\partial P}{\partial\theta} = \frac{\eta}{r^2}\left[\frac{\partial}{\partial r}\left(r^2\frac{\partial v_\theta}{\partial r}\right) + \frac{1}{\sin\theta}\frac{\partial}{\partial\theta}\left(\sin\theta\frac{\partial v_\theta}{\partial\theta}\right)\right.$$

$$\left. + \frac{1}{\sin^2\theta}\left(\frac{\partial^2 v_\theta}{\partial\phi^2}\right) + 2\frac{\partial v_r}{\partial\theta} - \frac{v_\theta}{\sin^2\theta} - \frac{2\cos\theta}{\sin^2\theta}\left(\frac{\partial v_\theta}{\partial\phi}\right)\right]$$

$$\frac{\partial P}{\partial\theta} = \frac{\eta}{r}\left[\frac{\partial}{\partial r}\left(r^2\frac{\partial v_\theta}{\partial r}\right) + \frac{\partial^2 v_\theta}{\partial\theta^2} + \frac{\partial}{\partial\theta}(\cot\theta v_\theta) + \frac{1}{\sin^2\theta}\left(\frac{\partial^2 v_\theta}{\partial\phi^2}\right)\right].$$

From (A7),

$$\frac{\partial^2 v_\theta}{\partial\phi^2} = 0$$

and using equation (A6),

$$\frac{\partial}{\partial\theta}\left(\frac{\partial v_\theta}{\partial\theta} + \cot\theta v_\theta\right) = \frac{\partial}{\partial\theta}(r\kappa(r)) = 0.$$

Thus, we want to solve

$$\frac{1}{\eta}\frac{\partial P}{\partial \theta}=\frac{1}{r}\frac{\partial}{\partial r}\left(r^2\frac{\partial v_\theta}{\partial r}\right)=2\frac{\partial v_\theta}{\partial r}+r\frac{\partial^2 v_\theta}{\partial r^2}. \tag{A9}$$

Boundary conditions of no slip:

$$v_\theta(a)=v_\theta(b)=0 \tag{A10}$$

give:

$$v_\theta=\frac{1}{2\eta}\frac{\partial P}{\partial \theta}\left[\frac{(r-a)(r-b)}{r}\right]. \tag{A11}$$

Equating (A7) and (A11),

$$\frac{1}{2\eta}\frac{\partial P}{\partial \theta}\left[\frac{(r-a)(r-b)}{r}\right]=-r\kappa(r)\cot\left(\frac{\theta}{2}\right).$$

Separating variables,

$$\frac{\partial P}{\partial \theta}\left[\cot\left(\frac{\theta}{2}\right)\right]^{-1}=2\eta\kappa(r)\left[\frac{r^2}{(b-r)(r-a)}\right]=\text{constant, say } k_2$$

$$\kappa(r)=-\frac{k_2}{2\eta}\left[1-\frac{a+b}{r}+\frac{ab}{r^2}\right].$$

Returning to (A5), above,

$$\int_0^{2\pi}\int_0^{\pi}\int_a^b(\nabla\cdot\mathbf{v})r^2\sin\theta\,dr d\theta d\phi=-f.$$

With

$$\nabla\cdot\mathbf{v}=\kappa(r)=-\frac{k_2}{2\eta}\left[1-\frac{a+b}{r}+\frac{ab}{r^2}\right]$$

$$k_2=\frac{3\eta f}{\pi(a-b)^3}.$$

Final results: Hele–Shaw flow

$$v_\theta=\frac{3f}{2\pi}\left(\frac{(r-a)(r-b)}{r}\right)\frac{\cot(\theta/2)}{(a-b)^3}. \tag{A12}$$

Note: no dependence on value of uniform viscosity.

$$\frac{\partial P}{\partial \theta}=\frac{3\eta f}{\pi(a-b)^3}\cot\frac{\theta}{2} \tag{A13}$$

$$P=\frac{3\eta f}{\pi}\frac{\ln\sin^2(\theta/2)}{(a-b)^3}+P_0 \tag{A14}$$

where P_0 is the pressure at $\theta=\pi$.

Miscellaneous results

Maximum velocity at $r_{\max}$ s.t. $\left.\frac{\partial v_\theta}{\partial r}\right|_{r_{\max}} = 0$

$$\left[1 - \frac{ab}{r_{\max}^2}\right] = 0$$

$$r_{\max} = (ab)^{1/2}$$

$$\mathbf{v}_{\max} = \frac{3f}{2\pi} \frac{\cot(\theta/2)}{(b-a)^3} [b^{1/2} - a^{1/2}]^2 \hat{\mathbf{e}}_\theta .$$

(This is for counterflow alone, obviously. Superposition of shear flow will shift the maximum.) Mean velocity

$$\bar{v}_\theta = \frac{\iint \mathbf{v} \cdot \mathbf{ds}}{\iint ds}$$

$$\bar{\mathbf{v}}_\theta = \frac{f}{2\pi} (b^2 - a^2)^{-1} \cot\left(\frac{\theta}{2}\right) \hat{\mathbf{e}}_\theta$$

$$\mathbf{v}_\theta = \left[3 \left(\frac{(r-a)(r-b)}{r}\right) \frac{b^2 - a^2}{(a-b)^3}\right] \bar{\mathbf{v}}_\theta .$$

Stresses

For the shear flow, in the same coordinate system as (A1). Evaluated at the base of the lithosphere $r = b$,

$$\sigma_{r\phi} = 3\eta \left(\frac{a^3}{b^3 - a^3}\right) \omega \sin\theta .$$

At the bottom of the asthenosphere $r = a$,

$$\sigma_{r\phi} = 3\eta \left(\frac{b^3}{b^3 - a^3}\right) \omega \sin\theta .$$

For the Hele–Shaw (return) flow, in the coordinate system of (A6), at the base of the lithosphere, $r = b$

$$\sigma_{r\theta} = -\left[\frac{3\eta f}{2\pi b (a-b)^2}\right] \cot\left(\frac{\theta}{2}\right).$$

At the base of the asthenosphere, $r = a$

$$\sigma_{r\theta} = -\left[\frac{3\eta f}{2\pi a (a-b)^2}\right] \cot\left(\frac{\theta}{2}\right).$$